

Molecular Dynamics Simulations of Classical Stopping Power

P. E. Grabowski, M. P. Surh, D. F. Richards, A. B. Langdon, F. R. Graziani, M. S. Murillo

August 19, 2013

Physical Review Letters

Disclaimer

This document was prepared as an account of work sponsored by an agency of the United States government. Neither the United States government nor Lawrence Livermore National Security, LLC, nor any of their employees makes any warranty, expressed or implied, or assumes any legal liability or responsibility for the accuracy, completeness, or usefulness of any information, apparatus, product, or process disclosed, or represents that its use would not infringe privately owned rights. Reference herein to any specific commercial product, process, or service by trade name, trademark, manufacturer, or otherwise does not necessarily constitute or imply its endorsement, recommendation, or favoring by the United States government or Lawrence Livermore National Security, LLC. The views and opinions of authors expressed herein do not necessarily state or reflect those of the United States government or Lawrence Livermore National Security, LLC, and shall not be used for advertising or product endorsement purposes.

Molecular Dynamics Simulations of Classical Stopping Power

Paul E. Grabowski, Michael P. Surh, David F. Richards, Paul E. Grabowski, Michael P. Surh, David F. Richards, David F. Richards, David F. Richards, Paul E. Grabowski, Michael P. Surh, David F. Richards, David F. Richards,

A. Bruce Langdon,² Frank R. Graziani,² and Michael S. Murillo^{1,*}

¹Computational Physics and Methods Group,

Los Alamos National Laboratory, Los Alamos, NM 87545, USA

²Lawrence Livermore National Laboratory, Livermore, CA 94550, USA

(Dated: August 14, 2013)

Abstract

Molecular dynamics can provide very accurate tests of classical kinetic theory; for example, unambiguous comparisons can be made for classical particles interacting via a repulsive 1/r potential. The plasma stopping power problem, of great interest in its own right, provides an especially stringent test of a velocity-dependent transport property. We have performed large-scale ($\sim 10^4$ – 10^6 particles) molecular dynamics simulations of charged-particle stopping in a classical electron gas that span the entire weak to strong intratarget coupling regimes. Projectile-target coupling is varied with projectile charge and velocity. Comparisons are made with disparate kinetic theories (both Boltzmann and Lenard-Balescu classes) and fully convergent theories to establish regimes of validity. We extend these various stopping models to improve agreement with the MD data and provide a useful fit to our results.

PACS numbers: 52.27.Gr,05.20.Dd,52.65.Yy,52.25.Dg

The nonequilibrium statistical mechanics of particles interacting via long-range forces is an outstanding challenge. Many-body simulations can provide insight into the wide range of complex behaviors that result [1–4]. Simulations are particularly valuable for model validation when precise data is lacking in high energy-density physics (HEDP) experiments [5, 6]. Whereas most transport phenomena represent averages over thermal velocities, charged particle stopping depends on a single projectile velocity. Thus stopping power provides a velocity-resolved probe of the underlying collision integrands and offers greater insight into the accuracy of energy and particle flow models, including temperature relaxation [7–9], diffusion [10, 11], and electrical and thermal conductivity [12, 13]. Improved knowledge of stopping power in HEDP environments also directly impacts ion-based fast ignition [14], alpha particle deposition in thermonuclear fuels [15], and heavy ion fusion [16].

Because molecular dynamics (MD) cannot include quantum scattering and recombination exactly, we consider a purely classical repulsive Coulomb system of a negatively-charged point projectile interacting with a one component electron gas target. Theoretical models can be formulated identically, so the MD provides a rigorous test of stopping power models [17]; insights can then be extrapolated to real matter. Within this system we vary both the intratarget and projectile-target coupling over large ranges to provide the greatest insight into the models. We vary the target temperature at fixed density to span weak to strong intratarget coupling, and we vary projectile charge and velocity to influence projectile-target coupling. In effect, we employ three independent coupling parameters.

In this letter, we compare theoretical models of charged-particle stopping [17–21] with numerically-exact, classical, nonrelativistic MD simulations. The underlying kinetic theories were chosen from the Lenard-Balescu (LB) class (weak scattering in a dense environment), the Boltzmann (B) class (strong scattering in a dilute environment), and convergent kinetic theories (CKT) [22]. We delimit regions of validity for these various models and quantify the importance of strongly-coupled nonlinear binary collisions and collective phenomena. We develop nonlinear screening models (beyond Debye-Hückel) to better describe these effects and obtain accurate expressions for classical stopping. We introduce a new formula for classical charged particle stopping which is more accurate over a larger parameter space compared to commonly used expressions.

Our simulations use the massively parallel MD code, ddcMD [23, 24], to treat long range forces. We varied the target temperature at fixed density $n_{\rm e}=1.03\times10^{20}~{\rm cm^{-3}}$ to obtain

three values for the intratarget coupling parameter $\Gamma = q_{\rm e}^2/(r_sT) = 0.1$, 1, 10. Here, $q_{\rm e}$ is the target charge, T is the target temperature in energy units, and $r_s = (4\pi n_e/3)^{-1/3}$ is the Wigner-Seitz radius. Projectile-target coupling was varied by selecting three projectile charges Z = -1, -2, -10 with projectile and target-particle masses consistent with the magnitude of the charge: $m = m_{\rm H}, m_{\rm He}, m_{\rm Ne}, m_{\rm e}$. Together these conditions define a matrix of nine physical conditions. For each of the nine cases, projectile velocities were selected in the range $v/v_{th} \sim 0.1$ –40, where $v_{th} = \sqrt{T/m_{\rm e}}$ is the thermal velocity of target particles.

Converged stopping behavior for the fastest projectiles considered required a numerical timestep of 10^{-5} to 10^{-4} fs. Long simulations were performed, typically 100 fs to relax transients followed by 300 fs $(172 \ \omega_p^{-1})$ of data collection. For fast projectiles, a weak Langevin thermostat (decay time 30–100 fs) was used to suppress target heating by the projectile; this did not affect the stopping. Fast charged particles generate wake potentials of large spatial extent, problematic for a finite simulation domain with periodic boundary conditions. Prior work [25, 26] corrected for the missing long-wavelength contributions using a model. To avoid such a model dependence we employed large cubic cells (10–100 Debye lengths on an edge, or roughly 64K–1M particles) and chose the initial projectile velocity to be a permutation of $\hat{v}=(1,\sqrt{\phi},\phi)$, with $\phi=(1+\sqrt{5})/2$, the golden ratio, minimizing overlap/interaction with periodic projectile-wakes. Our MD results are shown in the figures below. Multiple independent replicas establish error bars; nearly 900 simulations are included. We plot the stopping power, $-d\tilde{E}/dx$, versus velocity \tilde{v} , where $d\tilde{E}/dx = (dE/dx)(1+g)^{2/3}/(Z^2q_e^2/\lambda_D^2)$, $\tilde{v}=v/(v_{th}(1+g)^{1/3})$, $g=\sqrt{3}|Z|\Gamma^{3/2}$, and $\lambda_D=r_s/\sqrt{3}\Gamma$ is the Debye-Hückel (DH) screening length.

We find that the stopping rates determined by our MD simulations are accurately described by the expression

$$\frac{d\tilde{E}}{dx} \approx -R(w) \left[G(w) \ln \left(e^{1/2} + \frac{\alpha + w^2}{g_0} \right) + H(w) \right], \tag{1}$$

where

$$R(w) = \frac{[M_1 + bM_2(w)w^2](1+g)^{2/3}}{w^2(1+bw^2)},$$

$$M_1 = s \frac{\ln\left[1 + \alpha e^{-1/2}/g(1+aZ^2g)\right]}{\ln\left(1 + \alpha e^{-1/2}/g_0\right)},$$

$$M_2(w) = \frac{1}{s^2} \frac{\ln\left(1 + s^3w^3/g\right)}{\ln\left(1 + w^3/g_0\right)},$$

$$G(w) = \operatorname{erf}\left(\frac{w}{\sqrt{2}}\right) - \sqrt{\frac{2}{\pi}} w e^{-w^{2}/2},$$

$$H(w) = \frac{w^{4} \ln w}{12 + w^{4}} - \frac{w^{3}}{3\sqrt{2\pi}} e^{-w^{2}/2},$$
(2)

which is a generalization of a form given in Ref. [27]. Here, $\alpha = 4 \exp(-2\gamma)$, γ is Euler's constant, $0.577216\ldots$, $s = d(1+cg)^{1/3}$, $w = v/v_{th}s$, and the fit parameters are $a = 1.04102 \times 10^{-5}$, b = 0.183260, c = 0.116053, d = 0.824982, and $g_0 = 2.03301 \times 10^{-3}$. Equation (1) may be used for example to describe the light ionic component of heavy ion stopping power. Over our nine simulation conditions, this fit has a maximum and root mean square error of 0.03 and 0.005, respectively, in units of $Z^2q_e^2(1+g)^{2/3}/\lambda_D^2$.

Figure 1 compares Eq. (1) and our MD results to three models that are in wide use: the result from the NRL Plasma Formulary (NRL) [28], the Brown-Preston-Singleton (BPS) model [29], and the Li and Petrasso (LP) model [30]. We have evaluated the LP model with the u appearing in LP given by $\sqrt{v_{th}^2 + v^2}$ and the NRL model using the Coulomb logarithm $\Lambda = 23 - \ln[|Z|(T/\text{eV})^{-3/2}(n_e/\text{cm}^{-3})^{1/2}]$. For $\Gamma = 0.1$ and Z = -1 the BPS model works well, but NRL fails at high velocities, and LP suffers at the peak due to the use of a Heaviside theta function in its high-velocity correction. Other cases show larger deviations, particularly at low velocities when their Coulomb logarithms change sign. Only Eq. (1) matches the simulations for all conditions.

Figure 2 shows MD results for the four extreme limits of our nine cases; other cases give results between those shown. We compare the MD data with models of the LB class, which assume weak scattering with dynamical screening, thereby including many-body effects without invoking an ad hoc long-wavelength cutoff. This allows us to address three issues: the boundaries of a common LB-class model with respect to the three effective coupling parameters, the appropriate short-range cutoff, since the neglect of strong scattering in LB models leads to a divergence for classical systems, and the importance of dynamical screening. We will use these points for constructing improved models below. In Fig. 2 we plot

$$\frac{d\tilde{E}}{dx} = -\frac{2}{\pi\tilde{v}^2} \int_0^u d\tilde{\omega} \,\tilde{\omega} \int_0^Q dq \, q \, \frac{\text{Im}\left[\epsilon(q,\tilde{\omega})\right]}{|\epsilon(q,\beta\tilde{\omega})|^2},\tag{3}$$

where $q = k\lambda_D$, $\tilde{\omega} = \omega/(kv_{th})$, $u = v/v_{th}$, and Q gives the short-range cutoff. We evaluate the dielectric response using the random-phase approximation (RPA) [27]; setting β to zero or one selects static (SRPA) or dynamic (DRPA) screening, respectively. Traditionally, the

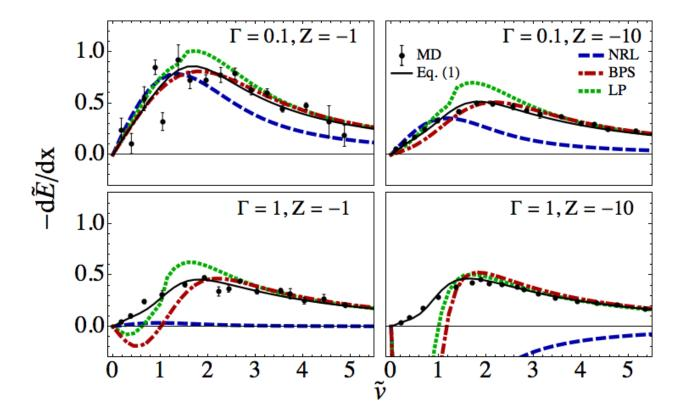


FIG. 1: Comparisons with three models (NRL, BPS, and LP) are made with the MD data for $\Gamma = 0.1, 1$ and two projectile charges Z = -1, -10. The fit of Eq. (1) is given by the thin black line.

cutoff Q is chosen to correspond to the distance of closest approach, $Q_{VIC} = \lambda_D T/Zq_e^2 = 1/g$, which we will refer to as the velocity independent cutoff (VIC). The VIC fails to produce the proper Bohr limit [31], $d\tilde{E}/dx = -\ln(u^3/g)/\tilde{v}^2$, so we also examine a velocity dependent cutoff (VDC) of the form $Q_{VDC} = Q_{VIC}(1+u^2)$ [25, 26]. From Fig. 2 we see that dynamical screening and a VDC are both needed to reproduce the MD data at high velocity. While the static screening model ($\beta = 0$) is accurate at low velocities for the weakest coupling, $\Gamma = 0.1$, it is not generally useful. As with the models in Fig. 1, the model given in Eq. (3) tends to fail when either (projectile-target or intratarget) coupling parameter is large, with the most egregious errors at low velocity.

We now turn to the B class of models, which employ a binary cross section, and thereby include strong scattering. Because the bare Coulomb cross section has a long-wavelength divergence, we show T-matrix results that include many-body screening effects. This is typically included [25] with a projectile-target interaction of the DH form $V_{pt}(r) = Ze^2 \exp(-r/\lambda_D)/r$.

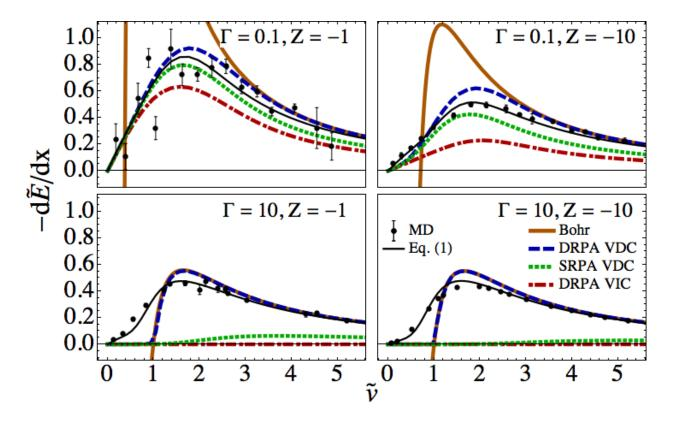


FIG. 2: Three LB-class stopping models, the Bohr model, and the MD data are shown for the four extreme cases in our data set. MD data (black points) are shown with five theory curves: the Bohr limit (solid orange), dynamic RPA velocity-dependent cutoff (dashed blue), dynamic RPA velocity-independent cutoff (dot-dashed red), and static RPA velocity-dependent cutoff (dotted green). The use of the velocity dependent cutoff with RPA is accurate everywhere except for small to moderate velocity. The fit of Eq. (1) is given by the thin black line.

We compute the cross section numerically (see Ref. [32]). This DH-based T-matrix model is limited to weakly coupled plasmas for two reasons: T-matrix assumes an effective binary scattering among uncorrelated particles, and DH screening is a linear, mean-field result. We remove the limitation of DH screening by computing the projectile-target interaction using the nonlinear Poisson-Boltzmann model and solving the hypernetted chain (HNC) equations [33] for the two-component plasma in the limit of one species (projectile) having vanishing concentration (see Ref. [34] for a similar usage of HNC). The nonlinear screening results are shown in Fig. 3, in which we see large deviations from DH for $\Gamma = 1, 10$. It is a limitation of the T-matrix formulation for strongly coupled plasmas that nonlinear screening potentials are not symmetric with respect to projectile and target. This leads to

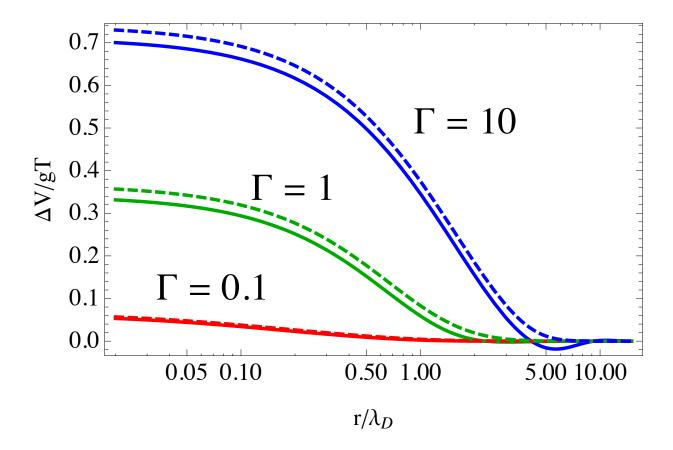


FIG. 3: Differences ΔV in nonlinear screening potentials from the linear mean field (DH), nonlinear mean field (PB, dashed), and beyond mean field (HNC, solid) are shown for three values of the Coulomb coupling constant.

an ambiguity in the potential used in the cross section calculation. In the nonlinear case, a projectile-target binary interaction is different depending on whether the target particle or the projectile is considered to be screened by other nearby target particles. We chose the former because it isolates the projectile exchanging energy with the target. However, neither viewpoint is correct, and when the two predictions differ significantly neither is accurate. In all cases the screening models are static and the T-matrix method cannot accurately describe the projectile velocity dependence. We have shown this to be important in Fig. 2; thus, in Fig. 4 we only show low velocity results. In general we see that the T-matrix results yield a considerable improvement over those in Fig. 2 at low velocity at all coupling parameters, a regime important for alpha particle stopping [15].

In the limits of low velocity and large projectile-target mass ratio, Dufty and collabora-

tors [35, 36] have shown an exact relationship between the stopping power and the diffusion coefficient, D: dE/dx = -vT/D. Of course, this formula only shifts the difficulty to D, which can be obtained from MD via the velocity autocorrelation function (VACF). Hughto $et\ al.$ [37] already did this calculation and provide a fit to their MD data ($\Gamma > 1$). We use their fit with the mass equal to our target particles [38, 39]. Low velocity stopping is fundamentally described by a non-binary, nonlinear model, since the VACF contains the many-body physics of a particle entrained in a collective background. Our results are shown in Fig. 4, which are in excellent agreement with the MD data at low velocity at $\Gamma = 1$ and 10, despite the fact that the D used was for an equal mass system. Because weakly coupled data was not used to train the fit, the deviations at $\Gamma = 0.1$ are not surprising.

To improve upon the poor velocity dependence of the T-matrix models, we also compare with CKT models [22]. Because of its partial success (see Fig. 2), we modified the DRPA VDC model to include static local field corrections (SLFC) $G_{ij}(k)$ for the projectile-target mixture, including both a $1 - G_{tt}(k)$ in the target dielectric function and a projectile-target factor $1 - G_{pt}(k)$ in the numerator of the integrand in Eq. (3): this serves to make the LB model convergent while also including many-body physics in the short-wavelength cutoff. We see in Fig. 4 that this greatly improves the low velocity results. Dynamic LFCs would be needed for the model to apply at all velocities. The Gould-Dewitt (GD) model [40], which constructs a CKT by employing both LB and B type features, is compared with the previously presented CKT BPS model. A model developed previously [25, 26, 41] that employs a velocity-dependent DH screening length is also considered, and we extend that to our nonlinear potentials. Our velocity-dependent scaling procedure scales all lengths Lin the potential as $L \to L\sqrt{1 + u^2(1 + \Gamma^3)^{1/4}}$, which empirically extends the prior work to strong coupling. The CKT comparisons are shown in Fig. 5 for the four corner cases of our data set. The models in this class agree very well at weak coupling. The GD model either offers no improvement over simpler models or does poorly. Comparison with the MD data reveals that the best model overall is our T-matrix model with HNC screening.

In summary, we have produced accurate molecular dynamics results for charged particle stopping using simulations that cover a broad range of projectile-target couplings, intratarget couplings and projectile velocities. These simulations employ orders of magnitude more particles than previous studies, allowing us to simulate long-wavelength wake structures. Our simulations utilized a purely classical plasma to allow for a model-independent comparison

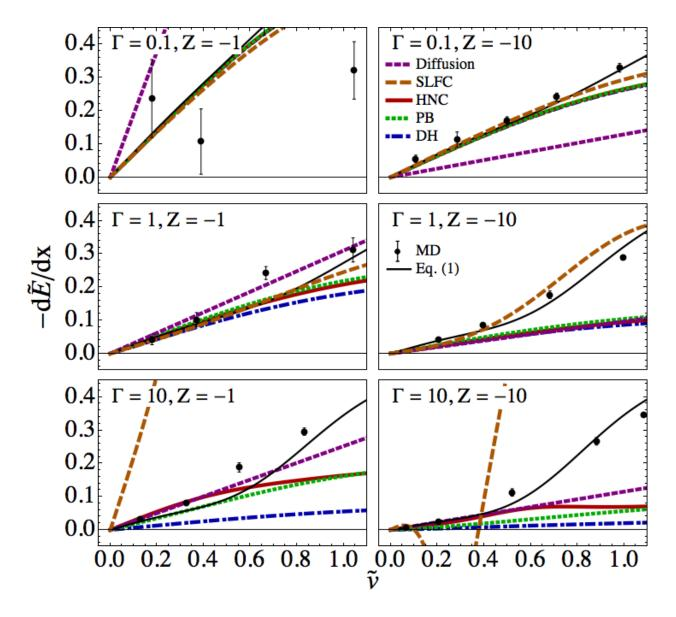


FIG. 4: T-matrix stopping power using three different screening potentials, Debye-Hückel (dot-dashed blue), Poisson-Boltzmann (dotted green), and HNC (solid red), shown with the diffusion model (short-dashed purple), SLFC (long-dashed orange), and MD data (points). The T-matrix model has the (known) defect of being inaccurate at high velocity, although the nonlinear screening potentials greatly improve the low velocity stopping power whenever the target-projectile coupling is large.

with theoretical models. We have provided a fit that accurately matches our MD results across the full range of temperature, velocity, and projectile charge we studied. We have compared our results with a very large range of differing theoretical models that originate from disparate branches of kinetic theory. Our data has allowed us to evaluate several

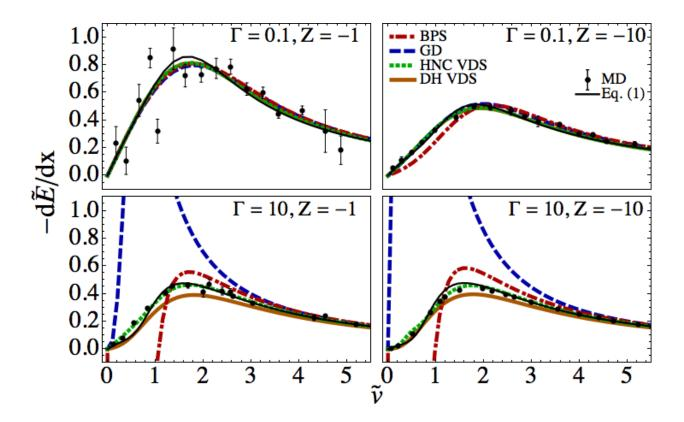


FIG. 5: A comparison of CKT models are shown, including BPS (dot-dashed red), GD (dashed blue), and improved T-matrix models that employ velocity-dependent screening lengths of two types (HNC (dotted green) and DH (solid orange)).

stopping power models that are in wide use. We find that models in the LB class yield accurate results for high velocity and any coupling parameter, provided that a velocity-dependent cutoff and dynamical screening are used. However, low velocity stopping is poorly predicted by LB models for the more strongly coupled cases, which can be improved by the inclusion of LFCs. In the B class we compared our data with T-matrix models, including a new model that includes nonlinear screening. While these models yield good results for low velocity, they are quite inaccurate at even moderate velocities; We find that while the nonlinear screening is a marked improvement, there are ambiguities in its implementation because there is no unique nonlinear potential to be used in a binary cross section. To bridge the gap between LB and B class models we also considered CKT models. We find that the CKT models are in excellent agreement with each other for weak coupling. For strong intratarget coupling, the GD and BPS models fail, with the best model being our T-matrix model that employs HNC screening and a velocity-scaled screening length. Finally, we have

compared our MD data with a stopping power model that relates stopping to diffusion and find very good agreement at low velocities, where that relationship should be accurate. Our MD results can readily distinguish among a very wide range of theoretical models.

The authors wish to thank Jim Glosli (LLNL) for very useful conversations. This work is performed under the auspices of the U. S. Department of Energy by Lawrence Livermore National Laboratory under Contract DE-AC52-07NA27344, and parts have been authored by employees of the Los Alamos National Security, LLC. (LANS), operator of the Los Alamos National Laboratory under Contract No. DE-AC52-06NA25396 with the U.S. Department of Energy. This work was funded by the Laboratory Directed Research and Development Program at LLNL under project tracking code 12-SI-005.

- * Electronic address: murillo@lanl.gov
- [1] Renato Pakter and Yan Levin. Topology of collisionless relaxation. Phys. Rev. Lett., 110: 140601, Apr 2013. doi: 10.1103/PhysRevLett.110.140601. URL http://link.aps.org/doi/10.1103/PhysRevLett.110.140601.
- [2] K. P. Driver and B. Militzer. All-Electron Path Integral Monte Carlo Simulations of Warm Dense Matter: Application to Water and Carbon Plasmas. PHYSICAL REVIEW LETTERS, 108(11), MAR 16 2012.
- [3] Peter Hartmann, Angela Douglass, Jorge C. Reyes, Lorin S. Matthews, Truell W. Hyde, Aniko Kovacs, and Zoltan Donko. Crystallization dynamics of a single layer complex plasma. *Phys. Rev. Lett.*, 105:115004, Sep 2010.
- [4] Michael S. Murillo and M. W. C. Dharma-wardana. Temperature relaxation in hot dense hydrogen. Phys. Rev. Lett., 100:205005, May 2008.
- [5] Miller, GH and Moses, EI and Wuest, CR. The National Ignition Facility: enabling fusion ignition for the 21st century. *NUCLEAR FUSION*, 44(12):S228–S238, DEC 2004.
- [6] Siegfried H. Glenzer and Ronald Redmer. X-ray thomson scattering in high energy density plasmas. Rev. Mod. Phys., 81:1625–1663, Dec 2009.
- [7] D. O. Gericke, M. S. Murillo, and M. Schlanges. Dense plasma temperature equilibration in the binary collision approximation. *Phys. Rev. E*, 65:036418, Mar 2002. doi: 10.1103/ PhysRevE.65.036418. URL http://link.aps.org/doi/10.1103/PhysRevE.65.036418.

- [8] Guy Dimonte and Jerome Daligault. Molecular-dynamics simulations of electron-ion temperature relaxation in a classical coulomb plasma. *Phys. Rev. Lett.*, 101:135001, Sep 2008.
- [9] Lorin X. Benedict, Michael P. Surh, John I. Castor, Saad A. Khairallah, Heather D. Whitley, David F. Richards, James N. Glosli, Michael S. Murillo, Christian R. Scullard, Paul E. Grabowski, David Michta, and Frank R. Graziani. Molecular dynamics simulations and generalized lenard-balescu calculations of electron-ion temperature equilibration in plasmas. *Phys. Rev. E*, 86:046406, Oct 2012. doi: 10.1103/PhysRevE.86.046406. URL http://link.aps.org/doi/10.1103/PhysRevE.86.046406.
- [10] Robert E. Rudd, William H. Cabot, Kyle J. Caspersen, Jeffrey A. Greenough, David F. Richards, Frederick H. Streitz, and Paul L. Miller. Self-diffusivity and interdiffusivity of molten aluminum-copper alloys under pressure, derived from molecular dynamics. *Phys. Rev. E*, 85:031202, Mar 2012. doi: 10.1103/PhysRevE.85.031202. URL http://link.aps.org/doi/10.1103/PhysRevE.85.031202.
- [11] L. Burakovsky, C. Ticknor, J. D. Kress, L. A. Collins, and F. Lambert. Transport properties of lithium hydride at extreme conditions from orbital-free molecular dynamics. *Phys. Rev. E*, 87:023104, Feb 2013. doi: 10.1103/PhysRevE.87.023104. URL http://link.aps.org/doi/ 10.1103/PhysRevE.87.023104.
- [12] M. P. Desjarlais, J. D. Kress, and L. A. Collins. Electrical conductivity for warm, dense aluminum plasmas and liquids. *Phys. Rev. E*, 66:025401, Aug 2002. doi: 10.1103/PhysRevE. 66.025401. URL http://link.aps.org/doi/10.1103/PhysRevE.66.025401.
- [13] Flavien Lambert, Vanina Recoules, Alain Decoster, Jean Clerouin, and Michael Desjarlais. On the transport coefficients of hydrogen in the inertial confinement fusion regime. *Physics of Plasmas*, 18(5):056306, 2011. doi: 10.1063/1.3574902. URL http://link.aip.org/link/?PHP/18/056306/1.
- [14] M. Roth, T. E. Cowan, M. H. Key, S. P. Hatchett, C. Brown, W. Fountain, J. Johnson, D. M. Pennington, R. A. Snavely, S. C. Wilks, K. Yasuike, H. Ruhl, F. Pegoraro, S. V. Bulanov, E. M. Campbell, M. D. Perry, and H. Powell. Fast ignition by intense laser-accelerated proton beams. *Phys. Rev. Lett.*, 86:436–439, Jan 2001.
- [15] JD Lindl, P Amendt, RL Berger, SG Glendinning, SH Glenzer, SW Haan, RL Kauffman, OL Landen, and LJ Suter. The physics basis for ignition using indirect-drive targets on the National Ignition Facility. PHYSICS OF PLASMAS, 11(2):339–491, FEB 2004.

- [16] DA Callahan-Miller and M Tabak. Progress in target physics and design for heavy ion fusion. PHYSICS OF PLASMAS, 7(5, Part 2):2083–2091, MAY 2000. 41st Annual Meeting of the Division of Plasma Physics of the American-Physical-Society, SEATTLE, WASHINGTON, NOV 15-19, 1999.
- [17] G Zwicknagel. Nonlinear energy loss of heavy ions in plasma. NUCLEAR INSTRUMENTS AND METHODS IN PHYSICS RESEARCH SECTION B-BEAM INTERACTIONS WITH MATERIALS AND ATOMS, 197(1-2):22–38, NOV 2002.
- [18] M. Ahsan Zeb, J. Kohanoff, D. Sánchez-Portal, A. Arnau, J. I. Juaristi, and Emilio Artacho. Electronic stopping power in gold: The role of d electrons and the h/he anomaly. *Phys. Rev. Lett.*, 108:225504, May 2012.
- [19] Zhang-Hu Hu, Yuan-Hong Song, and You-Nian Wang. Wake effect and stopping power for a charged ion moving in magnetized two-component plasmas: Two-dimensional particle-in-cell simulation. PHYSICAL REVIEW E, 82(2, Part 1), AUG 17 2010.
- [20] A. A. Solodov and R. Betti. Stopping power and range of energetic electrons in dense plasmas of fast-ignition fusion targets. PHYSICS OF PLASMAS, 15(4), APR 2008.
- [21] G Zwicknagel and C Deutsch. Correlated ion stopping in plasmas. *PHYSICAL REVIEW E*, 56(1, Part b):970–987, JUL 1997.
- [22] R.L. Liboff. Kinetic Theory: Classical, Quantum, and Relativistic Descriptions. Graduate Texts in Contemporary Physics. Springer, 2003. ISBN 9780387955513. URL http://books.google.com/books?id=h_E9pVIe38cC.
- [23] D. F. Richards, J. N. Glosli, B. Chan, M. R. Dorr, E. W. Draeger, J.-L. Fattebert, W. D. Krauss, T. Spelce, F. H. Streitz, M. P. Surh, and J. A. Gunnels. Beyond homogeneous decomposition: scaling long-range forces on massively parallel systems. In *Proceedings of the Conference on High Performance Computing Networking, Storage and Analysis*, SC '09, pages 60:1–60:12, 2009. ISBN 978-1-60558-744-8.
- [24] Frank R. Graziani, Victor S. Batista, Lorin X. Benedict, John I. Castor, Hui Chen, Sophia N. Chen, Chris A. Fichtl, James N. Glosli, Paul E. Grabowski, Alexander T. Graf, Stefan P. Hau-Riege, Andrew U. Hazi, Saad A. Khairallah, Liam Krauss, A. Bruce Langdon, Richard A. London, Andreas Markmann, Michael S. Murillo, David F. Richards, Howard A. Scott, Ronnie Shepherd, Liam G. Stanton, Fred H. Streitz, Michael P. Surh, Jon C. Weisheit, and Heather D. Whitley. Large-scale molecular dynamics simulations of dense plasmas: The Cimarron Project.

- HIGH ENERGY DENSITY PHYSICS, 8(1):105-131, MAR 2012.
- [25] G Zwicknagel, C Toepffer, and Reinhard P-G. Stopping of heavy ions in plasmas at strong coupling. *Physics Reports*, 309(3):117 208, 1999.
- [26] Günter Zwicknagel. Theory and Simulation of the Interaction of Ions with Plasmas: Nonlinear stopping, ion-ion correlation effects and collisions of ions with magnetized electrons. PhD thesis, Friedrich-Alexander Universitat Erlangen-Nurnberg, 2000.
- [27] Thomas Peter and Jürgen Meyer-ter Vehn. Energy loss of heavy ions in dense plasma. i. linear and nonlinear vlasov theory for the stopping power. *Phys. Rev. A*, 43:1998–2014, Feb 1991.
- [28] J.D. Huba. NRL Plasma Formulary. Naval Research Laboratory, 2009.
- [29] Lowell S. Brown, Dean L. Preston, and Robert L. Singleton Jr. Charged particle motion in a highly ionized plasma. *Physics Reports*, 410(4):237 333, 2005. ISSN 0370-1573.
- [30] Chi-Kang Li and Richard D. Petrasso. Charged-particle stopping powers in inertial confinement fusion plasmas. *Phys. Rev. Lett.*, 70:3059–3062, May 1993.
- [31] N. Bohr. On the decrease of velocity of swiftly moving electrified particles in passing through matter. *PHILOSOPHICAL MAGAZINE*, 30(175-80):581–612, JUL-DEC 1915.
- [32] S.A. Khrapak, A. V. Ivlev, G.E. Morfill, S.K. Zhdanov, and H.M. Thomas. Scattering in the attractive yukawa potential: application to the ion-drag force in complex plasmas. *Plasma Science*, *IEEE Transactions on*, 32(2):555–560, 2004. ISSN 0093-3813. doi: 10.1109/TPS. 2004.826073.
- [33] Setsuo Ichimaru, Hiroshi Iyetomi, and Shigenori Tanaka. Statistical physics of dense plasmas: Thermodynamics, transport coefficients and dynamic correlations. *Physics Reports*, 149(23): 91 – 205, 1987. ISSN 0370-1573.
- [34] Scott D. Baalrud and Jérôme Daligault. Effective potential theory for transport coefficients across coupling regimes. Phys. Rev. Lett., 110:235001, Jun 2013. doi: 10.1103/PhysRevLett. 110.235001. URL http://link.aps.org/doi/10.1103/PhysRevLett.110.235001.
- [35] JW DUFTY and M BERKOVSKY. ELECTRONIC STOPPING OF IONS IN THE LOW-VELOCITY LIMIT. NUCLEAR INSTRUMENTS & METHODS IN PHYSICS RESEARCH SECTION B-BEAM INTERACTIONS WITH MATERIALS AND ATOMS, 96(3-4):626-632, MAY 1995. Symposium in Honor of R H Ritchie on His 70th Birthday The Interaction of Swift Particles and Electromagnetic Fields with Matter, OAK RIDGE, TN, OCT 23-25, 1994.
- [36] JW Dufty, B Talin, and A Calisti. High Z ions in hot, dense matter. In ADVANCES IN

- QUANTUM CHEMISTRY, VOL 46: THEORY OF THE INTERACTION OF SWIFT IONS WITH MATTER, PT 2, volume 46 of ADVANCES IN QUANTUM CHEMISTRY, pages 293–305. ELSEVIER ACADEMIC PRESS INC, 2004.
- [37] J. Hughto, A. S. Schneider, C. J. Horowitz, and D. K. Berry. Diffusion of neon in white dwarf stars. PHYSICAL REVIEW E, 82(6, Part 2), DEC 1 2010. ISSN 1539-3755. doi: {10.1103/PhysRevE.82.066401}.
- [38] I. Binas and I. Mryglod. Mass-dependence of self-diffusion coefficients in disparate-mass binary fluid mixtures. CONDENSED MATTER PHYSICS, 12(4):647–656, 2009. ISSN 1607-324X. 3rd Conference on Statistical Physics, Lviv, UKRAINE, JUN 23-25, 2009.
- [39] Maria J. Nuevo, Juan J. Morales, and David M. Heyes. Mass dependence of isotope self-diffusion by molecular dynamics. *Phys. Rev. E*, 51:2026–2032, Mar 1995. doi: 10.1103/PhysRevE.51.2026. URL http://link.aps.org/doi/10.1103/PhysRevE.51.2026.
- [40] Harvey A. Gould and Hugh E. DeWitt. Convergent kinetic equation for a classical plasma. Phys. Rev., 155:68-74, Mar 1967. doi: 10.1103/PhysRev.155.68. URL http://link.aps.org/doi/10.1103/PhysRev.155.68.
- [41] Günter Zwicknagel and Claude Deutsch. Correlated ion stopping in plasmas. *Phys. Rev. E*, 56:970–987, Jul 1997. doi: 10.1103/PhysRevE.56.970. URL http://link.aps.org/doi/10.1103/PhysRevE.56.970.